



# Advanced oxidation protein products sensitized the transient receptor potential vanilloid 1 via NADPH oxidase 1 and 4 to cause mechanical hyperalgesia



Ruoting Ding<sup>a,1</sup>, Hui Jiang<sup>a,1</sup>, Baihui Sun<sup>b</sup>, Xiaoliang Wu<sup>a</sup>, Wei Li<sup>a</sup>, Siyuan Zhu<sup>a</sup>,  
Congrui Liao<sup>a</sup>, Zhaoming Zhong<sup>a,\*</sup>, Jianting Chen<sup>a,\*</sup>

<sup>a</sup> Department of Spinal Surgery, Nanfang Hospital, Southern Medical University, Guangzhou, Guangdong 510515, China

<sup>b</sup> Department of Plastic and Aesthetic Surgery, Nanfang Hospital, Southern Medical University, Guangzhou, Guangdong 510515, China

## ARTICLE INFO

### Article history:

Received 16 August 2016

Received in revised form

10 September 2016

Accepted 14 September 2016

Available online 17 September 2016

### Keywords:

Advanced oxidation protein products

Hyperalgesia

Dorsal root ganglion

NADPH oxidase

TRPV1

## ABSTRACT

Oxidative stress is a possible pathogenesis of hyperalgesia. Advanced oxidation protein products (AOPPs), a new family of oxidized protein compounds, have been considered as a novel marker of oxidative stress. However, the role of AOPPs in the mechanism of hyperalgesia remains unknown. Our study aims to investigate whether AOPPs have an effect on hyperalgesia and the possible underlying mechanisms. To identify the AOPPs involved, we induced hyperalgesia in rats by injecting complete Freund's adjuvant (CFA) in hindpaw. The level of plasma AOPPs in CFA-induced rats was 1.6-fold in comparison with what in normal rats ( $P < 0.05$ ). After intravenous injection of AOPPs-modified rat serum albumin (AOPPs-RSA) in Sprague-Dawley rats, the paw mechanical thresholds, measured by the electronic von Frey system, significantly declined. Immunofluorescence staining indicated that AOPPs increased expressions of NADPH oxidase 1 (Nox1), NADPH oxidase 4 (Nox4), transient receptor potential vanilloid 1 (TRPV1) and calcitonin gene-related peptide (CGRP) in the dorsal root ganglia (DRG) tissues. *In-vitro* studies were performed on primary DRG neurons which were obtained from both thoracic and lumbar DRG of rats. Results indicated that AOPPs triggered reactive oxygen species (ROS) production in DRG neurons, which were significantly abolished by ROS scavenger N-acetyl-L-cysteine (NAC) and small-interfering RNA (siRNA) silencing of Nox1 or Nox4. The expressions of Nox1, Nox4, TRPV1 and CGRP were significantly increased in AOPPs-induced DRG neurons. And relevant siRNA or inhibitors notably suppressed the expressions of these proteins and the calcium influxes in AOPPs-induced DRG neurons. In conclusion, AOPPs increased significantly in CFA-induced hyperalgesia rats and they activated Nox1/Nox4-ROS to sensitize TRPV1-dependent  $Ca^{2+}$  influx and CGRP release which led to inducing mechanical hyperalgesia.

© 2016 The Authors. Published by Elsevier B.V. This is an open access article under the CC BY-NC-ND license (<http://creativecommons.org/licenses/by-nc-nd/4.0/>).

## 1. Introduction

Hyperalgesia is a multifactorial situation caused by injury or dysfunction of the nervous system, this situation results in the increasing response to noxious stimuli [1]. Because pain hypersensitivity can persist long after the healing of the initial damage, it causes major health problems around the world [2]. Interestingly, many patients with systemic disorders, such as spinal cord injury (SCI) [3] and diabetes [4], suffer from hyperalgesia. Almost all of these patients accompany with oxidative stress when excessive amount of reactive oxygen species (ROS) are formed or

when the antioxidant capacity is decreased [5,6], and such imbalance may be a key factor to hyperalgesia [7]. The increasing knowledge about the molecular biology of ROS, such as hydrogen peroxide ( $H_2O_2$ ) and superoxide ( $O_2^{\bullet-}$ ), highlights their important role in their essential contribution to the development of pain hypersensitivity [8]. However, the source of hyperalgesia-related ROS and the underlying mechanisms still remain unclear.

Although there are numerous potential sources of ROS, nicotinamide adenine dinucleotide phosphate (NADPH) oxidase, the membrane-bound enzyme complexes, play a key role in the production of ROS [9]. In general, 4 rodent genes of the catalytic subunit Nox (Nox1–Nox4), which are expressed in a tissue-specific manner, have been identified [10]. For example, Nox1 is implicated in ROS generation in the development of thermal and mechanical hyperalgesia [11]. Nox2 is induced in spinal cord microglia cells after peripheral nerve injury and contributes to neuropathic pain

\* Corresponding authors.

E-mail addresses: [chenjt99@tom.com](mailto:chenjt99@tom.com) (Z. Zhong), [chenjt99@tom.com](mailto:chenjt99@tom.com) (J. Chen).

<sup>1</sup> These authors contributed equally to this work.

hypersensitivity [12]. Nox3 specially exists in the inner ear of mice and plays a crucial role in balance and gravity [13]. And Nox4 contributes to pain signaling after peripheral nerve injury. Nox4 mRNA has been detected in dorsal root ganglia, and Nox4-derived ROS production in the injured peripheral nerve stump essentially contributed to the initiation or maintenance of pain hypersensitivity [14].

Advanced oxidation protein products (AOPPs) are dityrosine-containing and cross-linking protein products, which are formed primarily as a consequence of oxidative stress [15]. AOPPs have been considered as a novel marker of oxidant-mediated protein damage. Recently, AOPPs have been recognized as a marker of oxidative stress and as a mediator of inflammation involved in the pathophysiology of many diseases [16–18]. It has been demonstrated that AOPPs are important source of ROS in vivo [19]. Furthermore, the roles of AOPPs in activating NADPH oxidase have been well documented. AOPPs can increase Nox1, Nox2 and Nox4 expression, and these are key regulatory subunits of NADPH oxidase [20].

The transient receptor potential vanilloid channel 1 (TRPV1) is a nonselective cation channel and is abundantly distributed in small and medium diameter primary afferent neurons of the dorsal root ganglion (DRG) [21]. Considerable evidences indicated that TRPV1 could be activated and potentiated by NADPH oxidase generated ROS [22]. Activation of TRPV1 enhanced intracellular calcium accumulation due to its permeability to  $\text{Ca}^{2+}$  [23], which was involved in many reactions (such as cellular viability, apoptosis, and physiological signal transduction). Meanwhile, enhanced TRPV1 caused the release of calcitonin gene-related peptide (CGRP) from DRG neurons, which played a key role in initiating neurogenic inflammation and leading to hyperalgesia [24].

Therefore, this study was conducted to examine whether AOPPs could cause hyperalgesia and the potential mechanisms. Herein, we first reported AOPPs increase in complete Freund's adjuvant (CFA)-induced hyperalgesia rats, and we also identified a potential role of AOPPs in activating TRPV1 via NADPH oxidase-dependent ROS production, which also mediated CGRP upregulation and calcium influx increase. These data provided new information for understanding the source of hyperalgesia-related ROS and the underlying mechanisms of AOPPs-induced hyperalgesia.

## 2. Materials and methods

### 2.1. Animals

Male Sprague-Dawley rats (initial weight 200–250 g, Animal Experiment Center, Southern Medical University, Guangzhou, China) were used in this study. Rats were housed 5 per cage under a standard 12 h/12 h light/dark cycle with food and water available ad libitum. Before any experimental procedures, rats were acclimated for 7 days. All experiments followed the recommendations of the International Association of Studies on Pain, and were approved by the Laboratory Animal Care and Use Committee of Nanfang hospital, Southern Medical University (NFYY-2014-86).

### 2.2. Chemicals and antibodies

The following chemicals and antibodies were obtained from Sigma-Aldrich (St. Louis, MO, USA): Complete Freund's adjuvant (CFA), rat serum albumin (RSA), hypochlorous acid (HOCl), amebocyte lysate assay kit, chloramine-T, acetic acid, 4% paraformaldehyde, bovine serum albumin (BSA), trypsin, collagenase type IA, DNase type IV, cytosine arabinoside, thiazolyl blue tetrazolium blue (MTT), dimethyl sulfoxide (DMSO), 2',7'-

dichlorofluorescein diacetate (DCFH-DA), phenylmethylsulfonyl fluoride (PMSF), protease and phosphatase inhibitors, Fura-2/AM, apocynin, N-acetyl-L-cysteine (NAC), and SB366791. Dulbecco's modified Eagle's medium (DMEM; 4.5 g/L glucose), fetal bovine serum (FBS), penicillin, streptomycin and glutamine were purchased from Gibco (CA, USA). Detoxi-Gel column and BCA Protein Assay Kit were purchased from Thermo Fisher Scientific (MA, USA).

The primary antibodies used in this study were rabbit anti-NADPH oxidase 1, anti-NADPH oxidase 2, anti-NADPH oxidase 4, rabbit anti-TRPV1, rabbit anti-calcitonin gene-related peptide (CGRP) and chicken anti-beta III Tubulin antibody and rabbit anti- $\beta$ -actin from Abcam (MA, USA). Secondary antibodies conjugated with FITC or Cy3 were purchased from Abcam (MA, USA).

### 2.3. Preparation of AOPPs-RSA and determination

As previously described, AOPPs-RSA were prepared with minor modifications [25]. In brief, 20 mg/mL of RSA was added to 200 mM of HOCl for 30 min at room temperature and dialyzed for 24 h against PBS at 4 °C to remove the free HOCl. Control incubation was performed in native RSA dissolved in PBS alone. All the preparations were passed through a Detoxi-Gel column to remove any contaminated endotoxin. Endotoxin levels were measured with an amebocyte lysate assay kit and were found to be below 0.025 EU/mL. To quantify AOPPs concentration [26], 200  $\mu$ L of sample or chloramine-T was placed in a 96-well plate, and then 20  $\mu$ L of acetic acid was added. SpectraMax M5 Multifunctional Microplate Reader (Molecular Devices, CA, USA) was used to measure the absorbance at 340 nm immediately. The content of AOPPs in the AOPPs-RSA was  $58.13 \pm 2.62 \mu\text{mol/g}$  protein versus  $0.22 \pm 0.03 \mu\text{mol/g}$  protein in unmodified RSA.

### 2.4. Animal experimental design

Hyperalgesia was induced by injecting subcutaneously an emulsion of 100  $\mu$ L of CFA 50% dissolved in PBS (sterilized) into the left hind paw, while the rats were under brief isoflurane anesthesia. Sham rats received a 100  $\mu$ L injection of PBS (sterilized) [27]. For characterization of paw withdrawal threshold, CFA group and corresponding PBS group ( $n=4$  rats/group) were tested 3 days before injection and in the time course experiment at days 0, 3, 6, 9, 12, 15, 18 and 21 after CFA injection. Plasma AOPPs concentration in the CFA model was measured after deeply anesthetized with pentobarbital sodium (150 mg/kg) at Day 21.

For AOPPs-induced hyperalgesia, the rats were randomly divided into 5 groups (5 rats per group): AOPPs-RSA group, PBS group, RSA group, apocynin group, and AOPPs-RSA+apocynin group. In our study, we injected AOPPs-RSA into healthy SD rats, according to plasma AOPPs concentration in the CFA model and our previous study [17,28]. AOPPs-RSA (50 mg/kg), RSA (50 mg/kg), and PBS (pH 7.4) were intravenously injected each day of the study, Antioxidant apocynin (50 mg/kg) was dosed by intragastric administration each day of the study duration. The basic threshold of each rat was tested 3 days before drugs were injected. After treatment, rats were tested on Days 0, 3, 6, 9, . . . , 27 and 30. The time interval was 2 days. Plasma and DRG tissues were obtained after deeply anesthetized with pentobarbital sodium (150 mg/kg) on Day 30.

### 2.5. Mechanical hyperalgesia assays

This study was performed at the same time of day and by an experimenter unaware of the treatment applied. Each rat was placed in a clear plastic chamber on an elevated wire grid and acclimated for at least 15 min to the testing environment prior to

the experiment. Withdrawal responses to mechanical stimuli were determined using an Electronic von Frey Anesthesiometer system (IITC Life Science, CA, USA). The electronic von Frey polypropylene tip was applied perpendicularly to the mid-plantar surface of the selected hind paw and the intensity of the stimulus was automatically recorded when the paw was flexed reflexively followed by a clear flinch response after paw withdrawal. All rats were tested 5 times, with an inter-test period of 15 min [29].

## 2.6. Immunofluorescence staining

Immunofluorescence staining of DRG slides was performed as previously described [30]. Briefly, rats were anesthetized with isoflurane and pentobarbital sodium (150 mg/kg) at Day 30. The lumbar DRGs (L4–6) were removed and postfixed in 4% paraformaldehyde overnight at 4 °C and then were transferred into 30% sucrose (in PBS) at 4 °C for at least 24 h. Samples were cryostat sectioned at a thickness of 14–16 μm and stored at –80 °C until use. Sections were permeabilized, blocked in 5% bovine serum albumin in PBS for 1 h at room temperature and then incubated overnight at 4 °C with the following antibodies: rabbit anti-Nox1 (1:500), rabbit anti-Nox2 (1:500), rabbit anti-Nox4 (1:500), rabbit anti-TRPV1 (1:500), rabbit anti-CGRP (1:500), and chicken anti-beta III Tubulin antibody (1:1000). After rinsing in PBS, slides were incubated with secondary antibodies conjugated with FITC (1:500) or Cy3 (1:200) for 2 h at room temperature. Then, reacted slides were mounted and cover slipped. Images were captured with an Olympus FluoView FV10i self-contained confocal laser scanning microscope system (Olympus America Inc., PA, USA).

## 2.7. Primary sensory neurons culture

DRG from thoracic and lumbar spinal cord of rats were minced in cold PBS and incubated for 60–90 min at 37 °C in DMEM (4.5 g/L glucose) containing (in mg/mL): 0.5 trypsin, 1 collagenase type IA, and 0.1 DNase type IV. Fetal bovine serum was added to neutralize trypsin. Neurons were pelleted, suspended in DMEM containing 10% fetal bovine serum, 100 U/mL penicillin, 0.1 mg/mL streptomycin, 2 mM glutamine. Cells were plated on polylysine-coated wells. Cytosine arabinoside (1 μM) was added to eliminate mitotic cells, which including Schwann cells and fibroblasts. Cultures were maintained at 37 °C in a water-saturated atmosphere with 5% CO<sub>2</sub> for 3 d prior to start of the experiment [31].

## 2.8. Cell viability (MTT) assay

To determine the cell viability after AOPPs-RSA treatment, we used the MTT viability assay [22]. DRG neurons were cultured with AOPPs-RSA at the concentration of 50, 100, 200, or 400 μg/mL for 6 h and replaced the medium with control medium containing MTT solution (5 mg/mL) in an amount equal to 10% of the culture volume. After incubation for 4 h, removed cultures and dissolved the resulting MTT formazan in DMSO. The absorbance was measured at a wavelength of 490 nm.

## 2.9. Small interfering RNA (siRNA) transfection

To introduce siRNA into rat DRG neurons, the cells were plated on 6-well plates at 90% confluence before transfection. Individual siRNAs (at 5 nM), lipofectamine 3000 and Opti-MEM were mixed and incubated at room temperature for 20 min siRNA– lipofectamine 3000 complexes were added to cells for 24 h and the medium was replaced by fresh serum DMEM medium after transfection. Nox1 siRNA (190372), Nox2 siRNA (189525) and Nox4 siRNA (190243) were purchased from Thermo Fisher Scientific (MA, USA). Experiments were performed 72 h after transfection.

Knockdown of Nox1, Nox2 or Nox4 was assessed by western blots assay [32].

## 2.10. Intracellular ROS measurement

The level of intracellular ROS was assessed by fluorescence microplate reader and confocal laser scanning microscope system with the probe 2', 7'-dichlorofluorescein diacetate (DCFH-DA), which oxidizes to fluorescent dichlorofluorescein (DCF) in the presence of ROS, as described previously [17]. Briefly, DRG neurons were suspended in DMEM at a given concentration of 10<sup>8</sup>/L. Each sample was incubated in 10 μM DCFH-DA for 30 min in darkness. The excitation and emission wavelengths were 488 nm and 525 nm, respectively. The resulting data were normalized using the control values.

## 2.11. Western blot analysis

Samples were homogenized in ice-cold RIPA buffer with 1 mM PMSF, protease, and phosphatase inhibitors and cleared by centrifugation (12,000 rpm, 4 °C, 10 min). The protein concentration in the supernatant was determined using the BCA Protein Assay Kit. Equivalent amounts of extracted proteins (50 μg) were separated by 10% or 12% SDS–polyacrylamide gel electrophoresis, then electro-blotted onto polyvinylidene difluoride membranes (Millipore, MA, USA). The membranes were blocked using 5% blocking buffer (5% BSA in Tris-buffered saline with 0.1% Tween 20) for 1 h at room temperature. Blots were incubated overnight at 4 °C with the following primary antibodies: rabbit anti-Nox1 (1:1000), rabbit anti-Nox2 (1:1000), rabbit anti-Nox4 (1:1000), rabbit anti-TRPV1 (1:1000), and rabbit anti-CGRP (1:1000). The membrane was washed 3 times with TBST for 10 min and followed by incubation with appropriate secondary antibody for 2 h, and then washed again 3 times with TBST. Relative levels of immunoreactivity were quantified using the Kodak *In-vivo* Imaging System (Kodak, NY, USA). Rabbit anti-β-actin (1:2000) was used as an internal control for the concentration of proteins loaded.

## 2.12. Measurement of intracellular free calcium

The DRG neurons were seeded in 96-well plates and loaded with 4 μM Fura-2/AM in loading buffer for 45 min at 37 °C in the dark, washed twice with the phosphate buffer, incubated for an additional 30 min at 37 °C to complete probe de-esterification. The groups were exposed to the stimulations. Fluorescence was detected by using a SpectraMax M5 Multifunctional Microplate Reader. The fluorescence at 505 nm was measured after excitation at 340 nm and 380 nm, respectively [33].

## 2.13. Statistical analysis

Analyses were performed with SPSS 20.0 (IBM, NY, USA) and GraphPad Prism 5 (GraphPad Software, CA, USA) software. Statistical data are presented as means ± SEM. Comparisons were analyzed with student *t*-test (2 groups only) or ANOVA followed by the Bonferroni post hoc tests analysis. A value of *P* < 0.05 was considered statistically significant.

# 3. Results

## 3.1. Plasma AOPPs increased in CFA-induced rats

We tested the paw withdrawal threshold and measured the concentration of plasma AOPPs in CFA-induced rats. As shown in Fig. 1A, the paw withdrawal threshold declined from Day 0

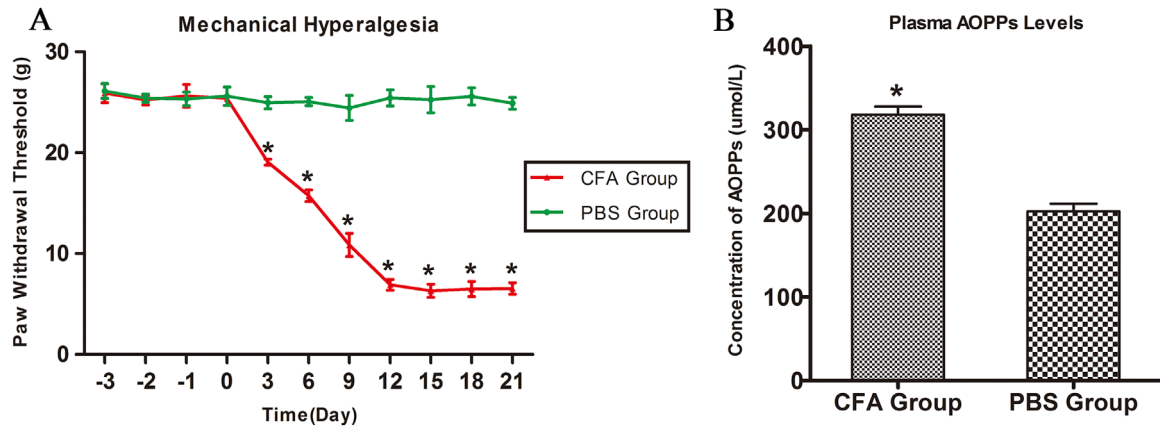


**Fig. 1.** The paw withdrawal threshold and the concentration of plasma AOPPs in CFA-induced rats. (A) Paw mechanical threshold was tested by the electronic von Frey system after different treatment. (B) The concentration of AOPPs in plasma was detected by chloramine-T method. Data represent mean  $\pm$  SEM of at least three independent experiments.  $n=4$  per group. \* $P < 0.05$  versus PBS group.

(25.38  $\pm$  0.13 g) to Day 12 (6.90  $\pm$  0.27 g) and remained at a low level until Day 21 (6.54  $\pm$  0.29 g). Fig. 1B indicated that the level of plasma AOPPs in CFA-induced rats was 1.6-fold in comparison with that in the PBS group ( $P < 0.05$ ). These data indicated that AOPPs were present in CFA-induced rats.

### 3.2. AOPPs induced mechanical hyperalgesia in SD rats

To elucidate whether AOPPs could induce mechanical hyperalgesia in SD rats, the electronic von Frey was used to measure the mechanical threshold of rats. As shown in Fig. 2A, the basic lines of paw mechanical threshold were determined by consecutive examination from 3 days before treatment. There was no significant difference among the 5 groups (the range was from 25.36  $\pm$  0.59 g to 26.63  $\pm$  0.31 g,  $P > 0.05$ ). Rats in these groups received different treatments and the paw mechanical threshold of each rat was tested every 3 days. After intravenous injection of AOPPs-RSA, the mechanical threshold significantly declined from Day 6 (19.45  $\pm$  0.51 g) to Day 27 (5.90  $\pm$  0.24 g) and remained a low level until Day 30 (5.22  $\pm$  0.33 g). In addition, we found that intragastric administration of apocynin notably improved mechanical hyperalgesia induced by AOPPs from Day 9. The weight of rats in each group was recorded in Fig. 2B, and there was no significant difference between each group (the range was from 225.00  $\pm$  4.21 g to 341.80  $\pm$  8.46 g,  $P > 0.05$ ). Plasma AOPPs levels were detected in each group. Fig. 2C indicated that plasma AOPPs levels increased in AOPPs-RSA group (363.79  $\pm$  3.39  $\mu$ mol/L) and AOPPs-RSA+apocynin group (362.03  $\pm$  2.27  $\mu$ mol/L).

### 3.3. AOPPs increased expression of Nox1, Nox4, TRPV1 and CGRP in vivo

Immunoreactivity of anti-Nox1, anti-Nox2, anti-Nox4, anti-TRPV1, and anti-CGRP was observed in sections of rat DRG (L4-L6) neurons that were co-stained with the neuronal marker,  $\beta$ -tubulin III. Fig. 3A and B revealed that Nox1 and Nox4 were markedly increased in AOPPs-RSA group compared with that in PBS group, and apocynin partly inhibited AOPPs-induced Nox1 and Nox4 expression. As shown in Fig. 3C, expression of TRPV1 increased in AOPPs-RSA group, and apocynin also inhibited TRPV1 expression. Meanwhile, increasing expression of CGRP was observed in AOPPs-treated rats but not in rats of control group and the expression level was alleviated by apocynin (Fig. 3D). To confirm our results, we used Western blot assays to measure the expression level of Nox1, Nox4, TRPV1, and CGRP in DRG tissues (L4-L6) of AOPPs-treated rats. Fig. 3E indicated that the level of Nox1 significantly

increased in AOPPs-RSA group. Meanwhile, the expression of Nox4 increased  $\sim$ 2-fold in AOPPs-RSA group, and its inhibitor, apocynin, reduced its expression level by almost 75%. The level of TRPV1 increased significantly  $\sim$ 2-fold in AOPPs-RSA group in comparison with that in the PBS group, and intragastric administration of apocynin efficiently reduced the expression of AOPPs-triggered TRPV1 by 50%. Furthermore, CGRP increased close to 2-fold in the AOPPs-RSA group compared with that in the PBS group, and were down-regulated by apocynin by approximately 60%. Notably, the expression of Nox2 which was tested by immunofluorescence staining or western blots had no significant difference between each group (Fig. S1).

### 3.4. AOPPs up-regulated Nox1 and Nox4 expression in DRG neurons

To investigate the effect of AOPPs-RSA on NADPH oxidase expression in rat DRG neurons, the cells were stimulated with increasing concentrations of AOPPs-RSA (0, 50, 100 and 200  $\mu$ g/mL) for different time (0, 15, 30, 60, 120 and 360 min). The protein levels of Nox1, Nox2 and Nox4 were analyzed by western blot from AOPPs-stimulated rat DRG neurons. The Nox1 and Nox4 protein level gradually increased after AOPPs stimulation at 0–200  $\mu$ g/mL (Fig. 4A and C). AOPPs-RSA stimulation also time-dependently induced Nox1 and Nox4 protein expression (Fig. 4D and F). As for protein expression of Nox2 (Fig. 4B and E), the results showed no significant difference at indicated concentrations or time durations as analyzed by Western blot. Next, we knocked down Nox1, Nox2 and Nox4 gene in DRG neurons, and Nox1, Nox2 or Nox4 siRNA transfection dramatically reduced AOPPs-induced Nox1, Nox2 or Nox4 expression in rat DRG neurons (Fig. 4G-I). These results indicate that up-regulation of Nox1 and Nox4 may be critical for AOPPs-mediated ROS production in rat DRG neurons.

### 3.5. AOPPs regulated DRG neurons to generate redundant ROS via NADPH oxidase pathway

Previous studies demonstrated that DRG neurons produced intracellular ROS under oxidative stress [34]. To determine whether AOPPs, as oxidative stress products, can cause redundant ROS accumulation inside DRG neurons, we examined intracellular ROS levels in AOPPs-treated DRG neurons. According to 6 h MTT test results (Fig. 5A), 400  $\mu$ g/mL AOPPs-RSA caused significant DRG neurons death (cell viability was 61.80  $\pm$  4.20%), while incubation in 0 to 200  $\mu$ g/mL AOPPs-RSA had little effects on cell fatality (cell viability was above 95%). Thus, we subjected DRG neurons cultures to increasing concentrations of AOPPs-RSA (0, 50, 100 and

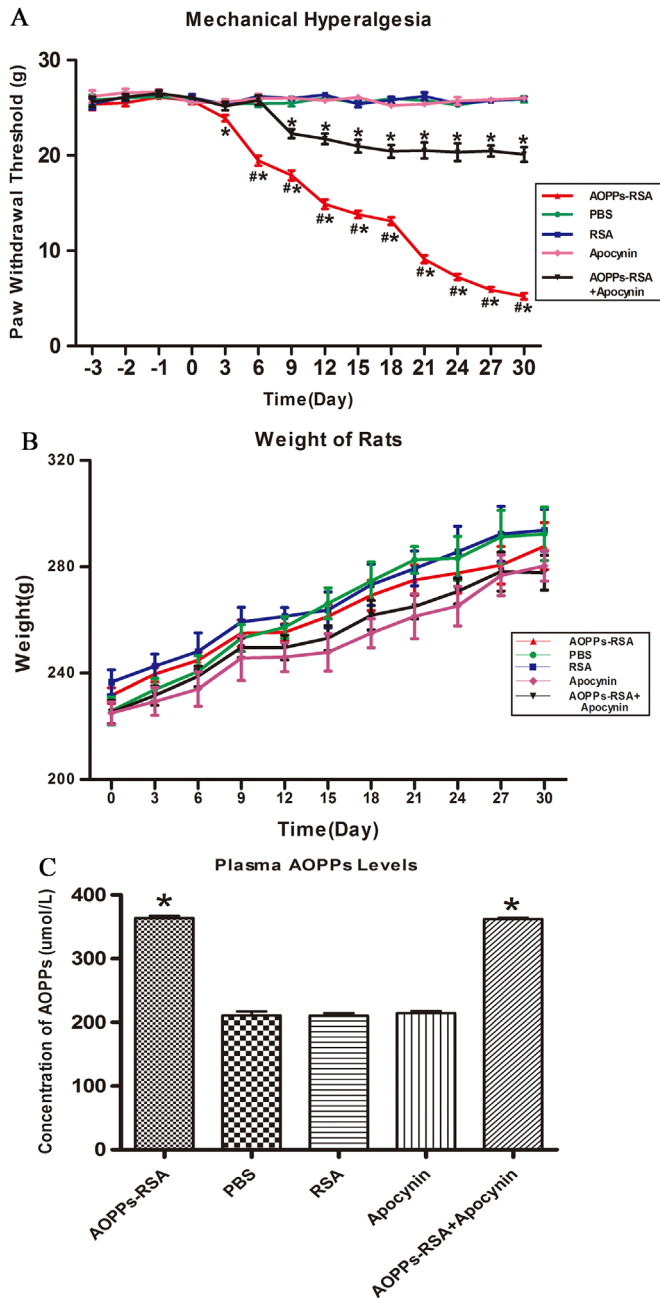


**Fig. 2.** AOPPs induced mechanical hyperalgesia in SD rats. (A) The basic lines of paw mechanical thresholds were tested 3 days continuously before treatment. Paw mechanical threshold was tested by the electronic von Frey system after different treatments. (B) The weight of each rat was measured every 3 days. (C) The concentration of AOPPs in plasma was detected by chloramine-T method. Data represent mean  $\pm$  SEM of at least 3 independent experiments.  $n=5$  per group. \* $P < 0.05$  versus PBS group. #  $P < 0.05$  versus AOPPs-RSA + apocynin group.

200  $\mu\text{g}/\text{mL}$ ) for different time (0, 5, 15, 30, 45, 60 and 120 min). ROS production was increased in DRG neurons cultured with AOPPs-RSA in a dose- and time-dependent manner (Fig. 5B and C). For further confirmation, ROS generation in DRG neurons cultured with control medium, RSA, AOPPs-RSA (200  $\mu\text{g}/\text{mL}$ ), AOPPs+siNox1, AOPP+siNox2, AOPP+siNox4, AOPP+NAC (2 mM, 2 h) was observed under a confocal laser scanning microscope system using DCFH-DA probe (Fig. 5E)..

To elucidate the function of NADPH oxidases in ROS generation, DRG neurons were respectively pre-treated with ROS scavenger NAC (2 mM, 2 h), Nox1 siRNA, Nox2 siRNA or Nox4 siRNA. After these treatments, DRG neurons were incubated with 200  $\mu\text{g}/\text{mL}$

AOPPs-RSA for 120 min. The level of ROS generation was significantly decreased in DRG neurons which were pretreated with NAC, Nox1 siRNA, or Nox4 siRNA separately (Fig. 5D), whereas Nox2 siRNA had little impact on the elevated levels of ROS. The results implied that AOPPs-RSA might elevate the levels of ROS in DRG neurons by activating Nox1 or Nox4.

### 3.6. AOPPs promoted CGRP release in DRG neurons through Nox1/Nox4-ROS-TRPV1

Western blot assay was used to verify the AOPPs-Nox1/Nox4-ROS-TRPV1-CGRP pathway. We stimulated DRG neurons with different concentrations of AOPPs-RSA (50, 100 and 200  $\mu\text{g}/\text{mL}$ ) for 6 h. The results showed that 50  $\mu\text{g}/\text{mL}$  AOPPs-RSA could significantly activate TRPV1, and the expression level of TRPV1 was elevated with the increasing concentration of AOPPs-RSA (Fig. 6A). However, the expression of CGRP did not increase until the concentration of AOPPs-RSA reached 100  $\mu\text{g}/\text{mL}$  (Fig. 6C). In addition, DRG neurons were stimulated by 200  $\mu\text{g}/\text{mL}$  AOPPs-RSA for different time durations (0, 15, 30, 60, 120 and 360 min). The expression of TRPV1 was up-regulated at least  $\sim 3$ -fold at 30 min in comparison with that at 0 min (Fig. 6B). The level of CGRP was increased close to 1.4-fold after 60 min (Fig. 6D)..

To further elucidate this pathway, DRG neurons were pretreated with Nox1 siRNA, Nox4 siRNA, NAC (2 mM) or SB366791 (a TRPV1 inhibitor, 1  $\mu\text{M}$ ) [35] before AOPPs-RSA (200  $\mu\text{g}/\text{mL}$ , 6 h) treatment. Our previous results indicated that Nox2 was not activated in AOPPs-induced ROS generation, so we did not use Nox2 siRNA in the transfection experiments. We found that the expressions of TRPV1 and CGRP were significantly decreased under these conditions (Fig. 6E). These results indicated that Nox1 and Nox4 participated in AOPPs-mediated TRPV1 and CGRP expression in rat DRG neurons observed in vitro.

### 3.7. AOPPs induced calcium influxes through activating TRPV1 channel

ROS increase intracellular free calcium by acting specifically on TRPV1 [22]. AOPPs -treated DRG neurons (200  $\mu\text{g}/\text{mL}$ , 2 h) showed more calcium influxes comparing to those in the control group (Fig. 7A). We further assessed calcium fluxes in DRG neurons which were pretreated with Nox1 siRNA, Nox4 siRNA, NAC (2 mM, 2 h), or SB366791 (1  $\mu\text{M}$ , 2 h) and then incubated with 200  $\mu\text{g}/\text{mL}$  AOPPs-RSA for 2 h. Fig. 7B showed that, comparing with the control group, despite of the fact that the concentration of intracellular calcium were higher in AOPPs+siNox1 group, AOPPs+siNox4 group and AOPPs+NAC group, these inhibitors could efficiently decrease the concentration of intracellular free calcium which was induced by AOPPs..

## 4. Discussion

Our study identified advanced oxidation protein products (AOPPs), a novel marker of oxidative stress, increased in complete Freund's adjuvant (CFA)-induced hyperalgesia model. To our knowledge, this is the first evidence for a function of AOPPs in a pathophysiological process implicating the nervous system and, in particular, hyperalgesia pathogenesis.

In 1996, the first report of AOPPs was made by Witko-Sarsat after the discovery of AOPPs in the plasma of uremic patients receiving maintenance dialysis [15]. Increasing evidences suggested that the formation and accumulation of plasma AOPPs served as pathogenic mediators that participated in various diseases, such as diabetes [16,36], coronary artery disease [18], cancer [37], liver cirrhosis [38], and chronic inflammatory bowel disease (IBD) [17].

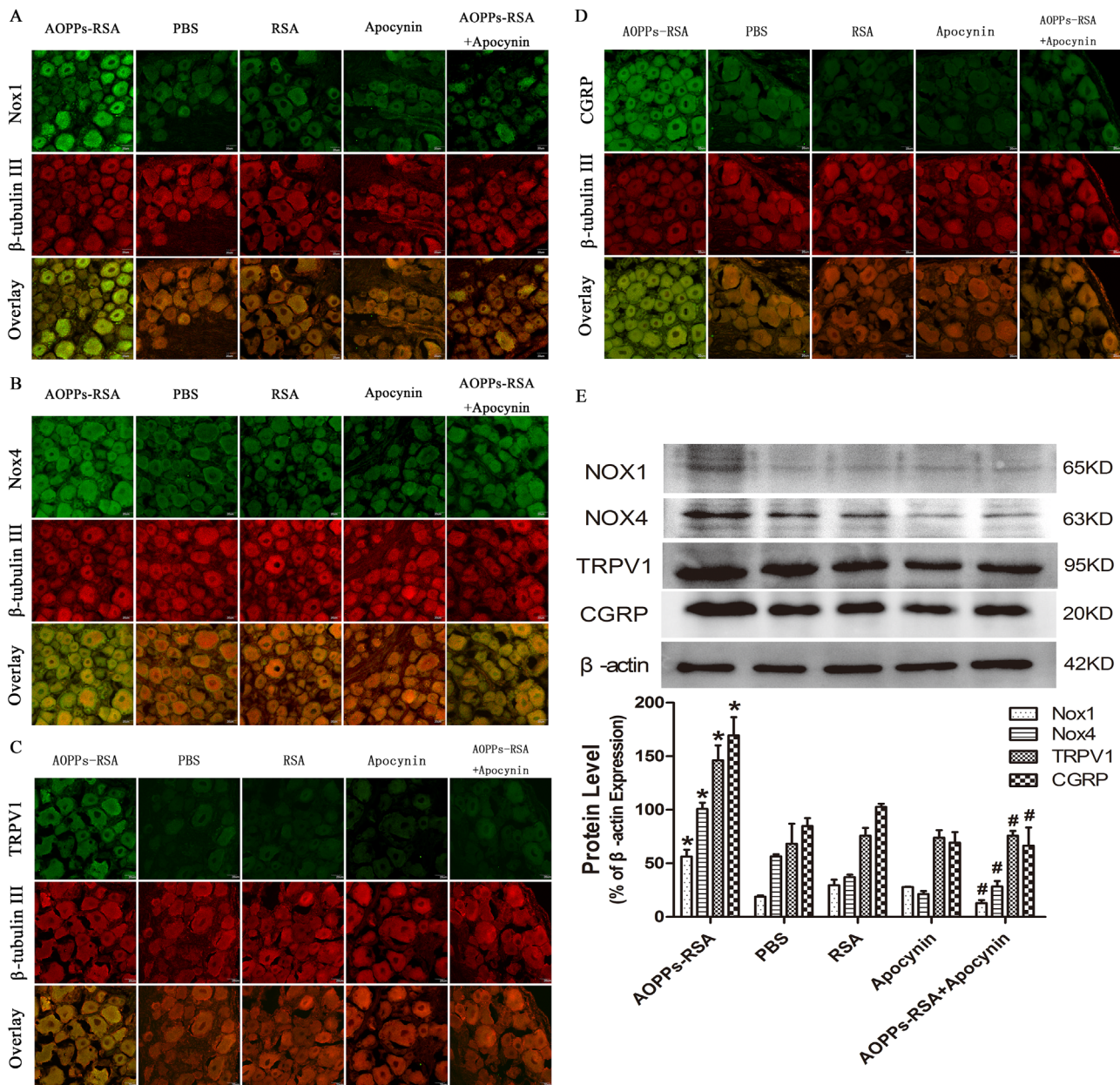


**Fig. 3.** Expression levels of Nox1, Nox4, TRPV1 channel and CGRP were detected in DRGs (L4–L6) in rats. (A–D) Immunofluorescence staining of DRGs in different groups, the target protein (Nox1, Nox4 TRPV1 and CGRP) was stained green, while  $\beta$ -tubulin III was red. (E) Expression levels of Nox1, Nox4, TRPV1, and CGRP in DRGs tissues (L4–L6) were detected by Western blotting. Data represent mean  $\pm$  SEM of at least 3 independent experiments.  $n=5$  rats per group. scale bar, 20  $\mu\text{m}$  \* $P < 0.05$  versus AOPPs-RSA group. #  $P < 0.05$  versus PBS group.

CFA-induced pain model is commonly used to study hyperalgesia [27]. However, little is known about the relationship between AOPPs and hyperalgesia. First, we detected the plasma concentration of AOPPs in the CFA-induced rats. Our results indicated that plasma AOPPs increased about 1.6-fold in comparison with that in normal rats. These results offered a reliable evidence for our follow-up studies about intravenous injection of AOPPs. Meanwhile, these showed that AOPPs might participate in the hyperalgesia process, which highlights the urgent need to understand whether AOPPs can induce the hyperalgesia and the underlying mechanisms.

We then wondered whether AOPPs could induce mechanical hyperalgesia. The paw mechanical threshold showed a tremendous decline from Day 6 to Day 27 and remained at a low level until Day 30 in AOPPs-induced rats. We also detected plasma AOPPs level in rats at Day 30, and the results suggested that

hyperalgesic efficacy of AOPPs was due to its biological effects. Interestingly, we found that the paw mechanical threshold of AOPPs-induced rats accorded with that of the CFA-induced rats, in which the plasma AOPPs concentration was 1.6 times compared with that in the PBS group. These data further reinforced the hypothesis of a potential role for AOPPs in the hyperalgesia processes.

Next, we investigated the possible involvement of TRPV1 in AOPPs-induced hyperalgesia processes. Previous theories established that peripheral TRPV1 primarily mediated thermal hyperalgesia. But recent studies have demonstrated that TRPV1 channel in DRG neurons mediated not only thermal hyperalgesia but also mechanical hyperalgesia [39–42]. Among TRP channels, the transient receptor potential ankyrin-1 (TRPA1) and TRPV1 are essential and widely studied molecular sensors and mediators of pain signals in DRG neurons. It is well documented that most if not all

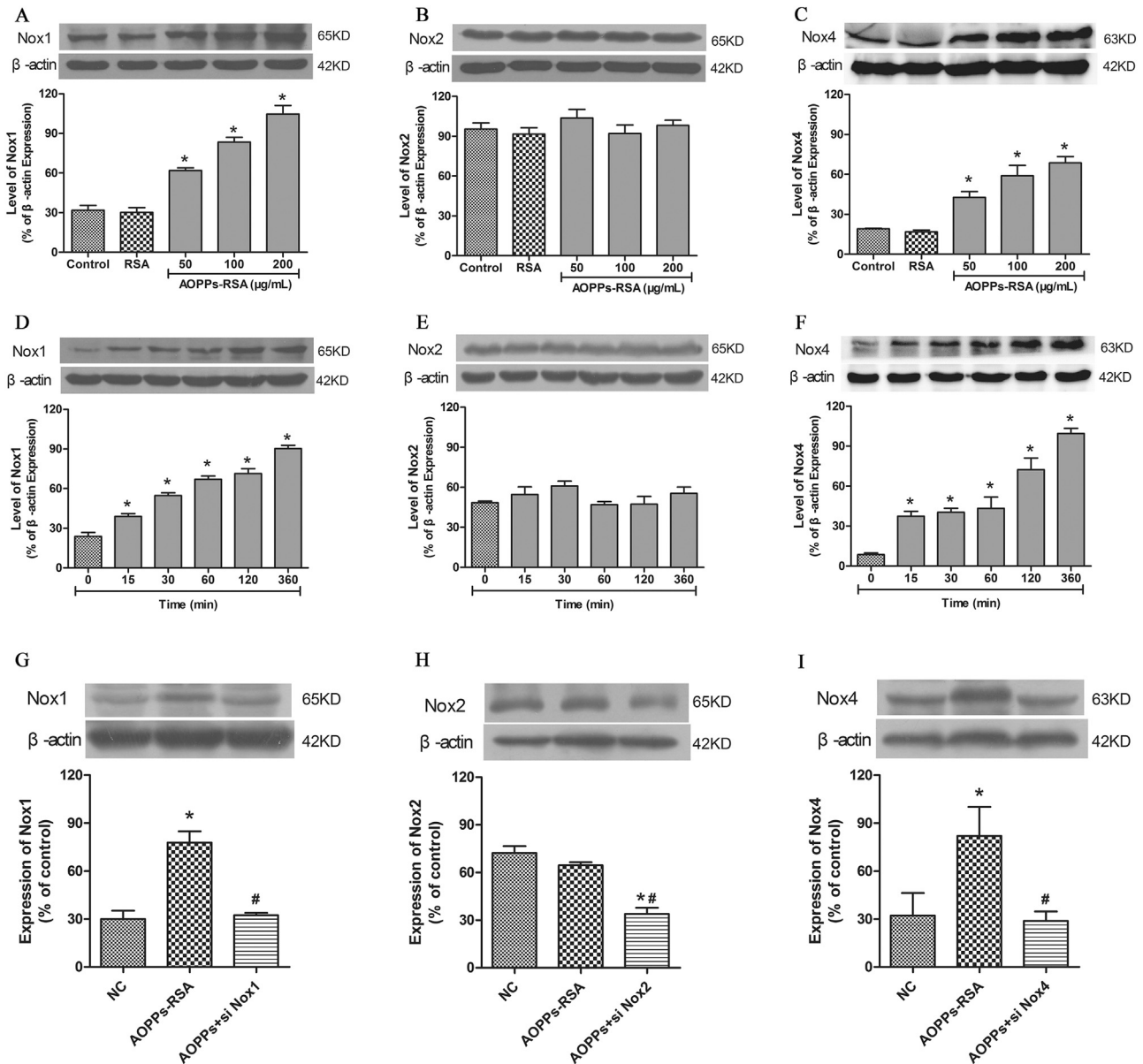


**Fig. 4.** The expression of NADPH oxidase in DRG neurons. (A, C) The levels of Nox1 and Nox4 were up-regulated significantly in DRG neurons incubated with AOPPs-RSA in indicated concentrations. (B) Indicated concentrations of AOPPs-RSA could not significantly up-regulate the expression of Nox2. (D, F) The levels of Nox1 and Nox4 were up-regulated significantly in DRG neurons incubated with 200 μg/mL AOPPs-RSA in different time durations. (E) The expression of Nox2 had no significant difference between indicated time durations in 200 μg/mL AOPPs-RSA-induced DRG neurons. (G–I) After Nox1 siRNA, Nox2 siRNA or Nox4 siRNA pretreatment, cells were stimulated with or without AOPPs-RSA (200 μg/mL) for 6 h, bar graph showed quantitative analysis of Nox1, Nox2 and Nox4. Data represent mean ± SEM of at least 3 independent experiments. \* $P < 0.05$  versus Control (0) group. #  $P < 0.05$  versus AOPPs-RSA group.

TRPA1<sup>+</sup> DRG neurons co-express TRPV1 [43]. There are abundant literatures on the functional effects of oxidative stress modification on TRPV1 channels [22,44], but little information regarding the role of AOPPs in the activation of TRPV1 channels. Herein, our immunofluorescence results confirm that TRPV1 is up-regulated *in vivo*, suggesting that AOPPs enhance TRPV1 expression resulting in mechanical hyperalgesia. On the other hand, we explored the involvement of TRPV1 in the regulation of this mechanism in primary cultured DRG neurons. We found that AOPPs could increase levels of TRPV1, which played a key role in the regulation of CGRP and intracellular calcium. However, we still cannot confirm that TRPV1 channel is the only TRP family that is activated. Further investigation is required to define the specificity.

As previously reported, emerging studies pointed the oxidative stress, especially the production of ROS, as key up-regulated TRPV1 mediators in a variety of pathologies [34], including pain

processes [7,8]. AOPPs can indirectly sensitize NADPH oxidase to cause ROS overproduction in many kinds of cells [17,45–48]. Herein, we stimulated DRG neurons with AOPPs-RSA at different concentrations and for different time durations. This study first demonstrated that AOPPs could trigger DRG neurons to generate abundant ROS. In contrast to the historical view that ROS are merely harmful, it is now clear that ROS can function as specific regulators of intracellular signaling pathways [49].

Moreover, we also need to figure out the source of ROS. Notably, Nox enzymes are distinct from most other ROS sources in that ROS generation is their major function but not a byproduct of other biological reactions [2]. We highlighted the specific role of Nox1, Nox2 and Nox4 in AOPPs-induced signaling. Our results showed that in cultured primary DRG neurons, AOPPs could significantly up-regulate Nox1 and Nox4. Whereas, they had little impact on the regulation of Nox2, which is considered

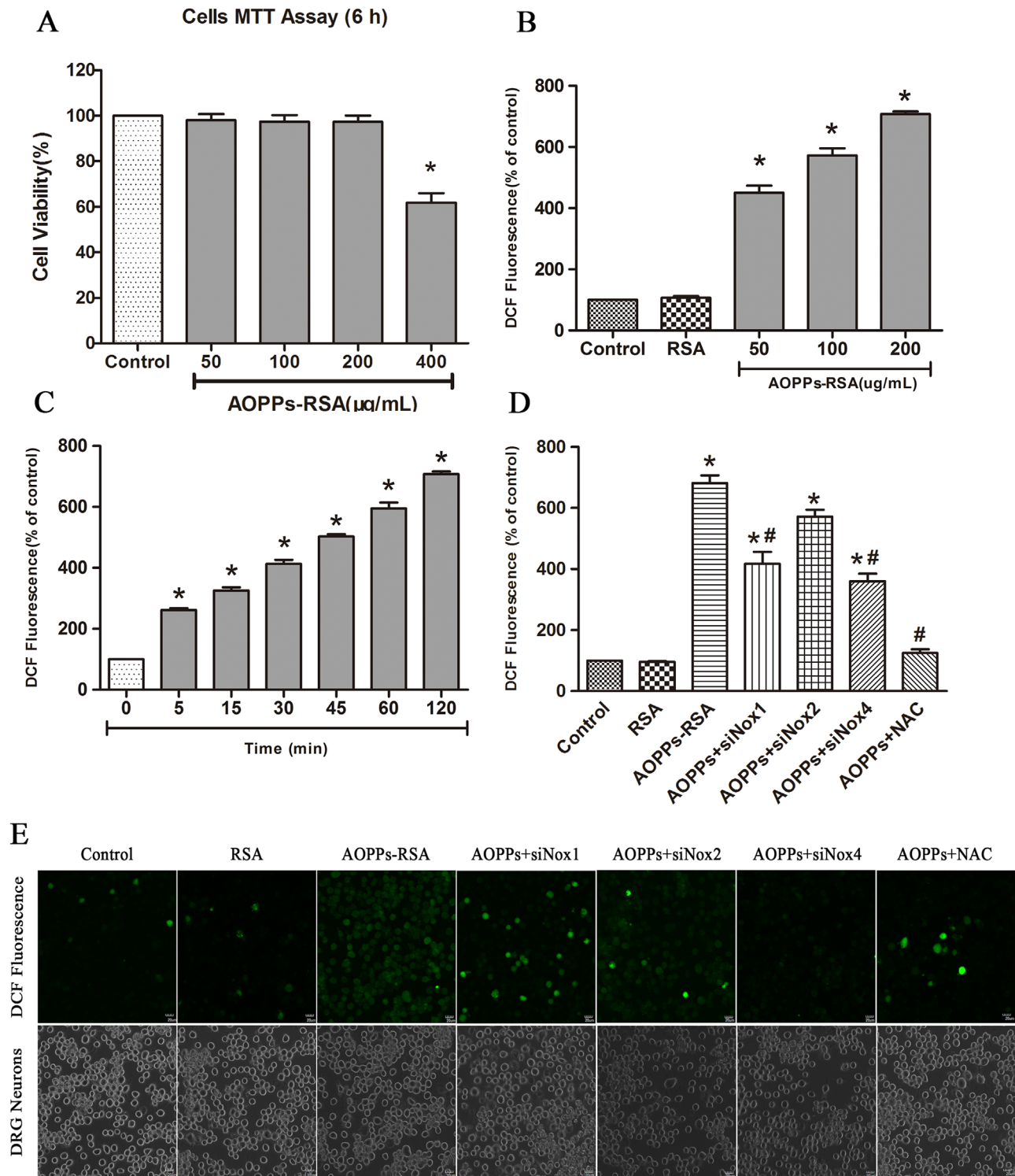


**Fig. 5.** AOPPs challenge increased reactive oxygen species (ROS) generation in DRG neurons via NADPH oxidase. (A) Viability of DRG neurons treated with AOPPs in different concentrations after cultured for 6 h. (B) DRG neurons were cultured as control cells, RSA group or with indicated concentration of AOPPs-RSA as AOPPs group for 2 h. (C) DRG neurons were incubated with 200  $\mu\text{g}/\text{mL}$  AOPPs-RSA for indicated time. (D) DRG neurons were treated with AOPPs-RSA (200  $\mu\text{g}/\text{mL}$ ) with or without Nox1 siRNA, Nox2 siRNA, Nox4 siRNA or NAC (2 mM, 2 h). AOPPs-induced ROS production was significantly diminished by NAC and Nox1 siRNA, Nox4 siRNA. (E) DRG neurons were cultured with control medium, RSA, AOPPs-RSA (200  $\mu\text{g}/\text{mL}$ ), AOPPs+siNox1, AOPPs+siNox2, AOPPs+siNox4, AOPPs+NAC for 120 min. Confocal laser scanning microscope system was used to visualize ROS generation in DRG neurons with the use of DCFH-DA. Data represent mean  $\pm$  SEM of at least 3 independent experiments. Scale bar, 20  $\mu\text{m}$ . \* $P < 0.05$  versus control (0) group. #  $P < 0.05$  versus AOPPs-RSA group.

predominantly expressed in glial cells and neutrophils [2]. Our present findings did not support the role of Nox2 in our AOPPs-induced molecular pathway, but they might be attributed to the close proximity between Nox1/Nox4 and the target molecule identified in this study, which enables direct interaction and

modulation of TRPV1 activity in DRG neurons. To best illuminate Nox1/Nox4-ROS-TRPV1 pathway, we used a series of siRNAs and inhibitors, such as siRNA Nox1, siRNA Nox4, NAC and SB366791. Collectively, these data first suggested that AOPPs might act as a key mediator for activating Nox1 and Nox4, and were necessary in



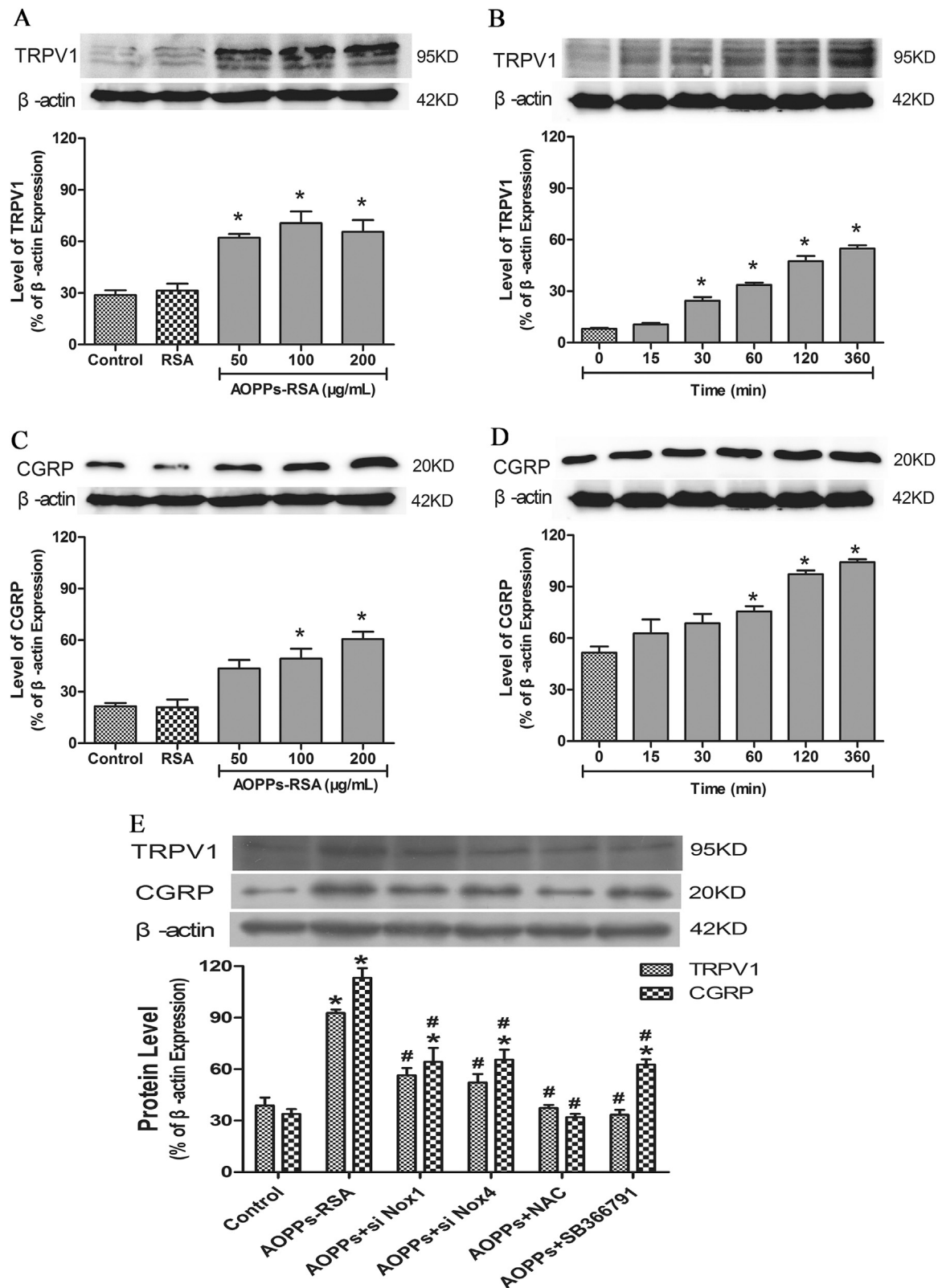


**Fig. 6.** The expression of related proteins in DRG neurons. (A–D) The levels of TRPV1 and CGRP were up-regulated significantly in DRG neurons incubated with AOPPs-RSA in indicated concentrations and time durations. (E) DRG neurons were incubated with AOPPs-RSA (200 μg/mL) with or without pretreatment with Nox1 siRNA, Nox4 siRNA, NAC (2 mM), or SB366791 (1 μM) for 6 h. The expression of TRPV1 and CGRP could be triggered by AOPPs, meanwhile, inhibited by these siRNAs or inhibitors. Data represent mean ± SEM of at least 3 independent experiments. \* $P < 0.05$  versus Control (0) group. #  $P < 0.05$  versus AOPPs-RSA group.

the process of Nox1/Nox4-derived ROS [50], they promoted redundant ROS, and in final, led to activating TRPV1 channel.

In addition, we found that  $Ca^{2+}$  influx happened via the

activation of TRPV1 channels under the condition of AOPPs treatment. Intracellular  $Ca^{2+}$  pools play an important role in cellular activities. Increases in  $Ca^{2+}$  concentration may conduce to

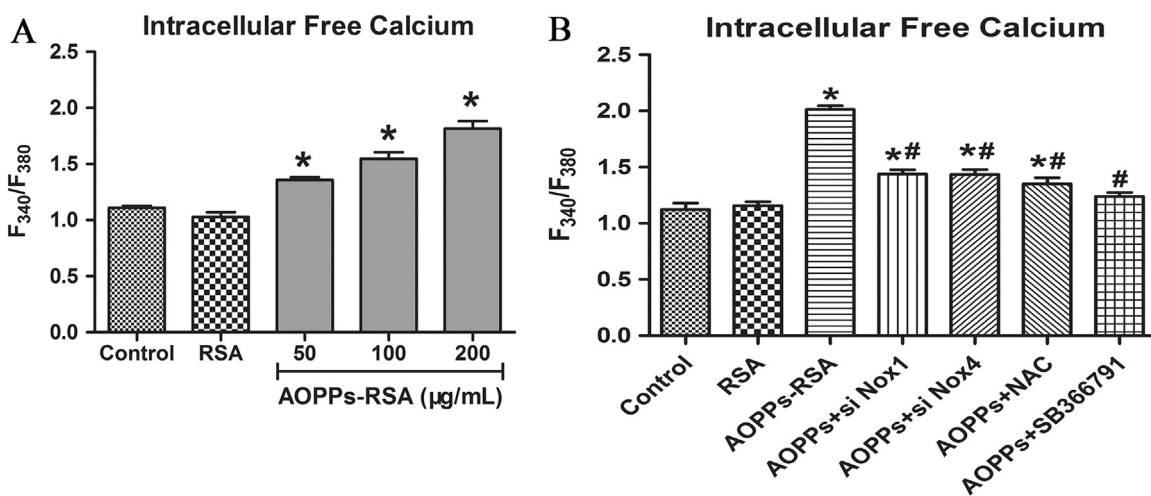


**Fig. 7.** Intracellular free calcium was detected by Fura-2/AM. (A) The levels of calcium were shown in  $F_{340}/F_{380}$ . (B) DRG neurons were incubated with AOPPs-RSA (200  $\mu\text{g}/\text{mL}$ ) with or without Nox1 siRNA, Nox4 siRNA, NAC (2 mM, 2 h), or SB366791 (1  $\mu\text{M}$ , 2 h).  $F_{340}/F_{380}$  was used to indicate intracellular free calcium. Data represent mean  $\pm$  SEM of at least 3 independent experiments. \* $P < 0.05$  versus Control group. #  $P < 0.05$  versus AOPPs-RSA group.

membrane depolarization [51], initiation of phosphorylation of membrane proteins that will enhance channel potency, and activation of a variety of intracellular enzymes [52]. Previous studies have shown that the intracellular  $\text{Ca}^{2+}$  influx into DRG neurons through activation of TRPV1 channels played a key role in neurotransmitter release and pain hypersensitivity [21]. Hence, we provided the novel finding that AOPPs potentially increased intracellular calcium by Nox1/Nox4-ROS mediated TRPV1 channel activation.

Finally, we detected immunoreactivity of CGRP in DRG tissues of rats and in the AOPPs-treated DRG neurons, the results indicated that AOPPs-induced CGRP release depended on the presence of TRPV1 channel. It has been ascertained that calcitonin gene-related peptide (CGRP), a 37-amino-acid peptide, is widespread in the neural systems [53]. CGRP is synthesized and stored in sensory neurons and can be released from both their central and peripheral axons [24]. Considerable evidences indicated that the release of CGRP from sensory nerve terminals played a key role in hyperalgesia [54,55]. It is well established that the synthesis and release of CGRP were regulated by the activation of TRPV1 [56]. On the other hand,  $\text{Ca}^{2+}$  released from intracellular stores probably contributes to the CGRP release [57]. Although our results suggested that AOPPs could sensitize TRPV1 to enhance CGRP release and cause mechanical hyperalgesia, we cannot exclude the possibility that AOPPs also sensitizes other cell types to enhance nociception.

In summary, our study provided for the first time that plasma AOPPs were increased in CFA-induced hyperalgesia rats. We identified a novel mechanism by which AOPPs sensitized TRPV1 to induce sustained mechanical hyperalgesia. Sensitization required activation of Nox1/Nox4 and was probably mediated by direct generating ROS to enhance channel gating. AOPPs-induced sensitization of TRPV1 caused intracellular  $\text{Ca}^{2+}$  increasing, enhanced CGRP release, and exacerbated pain hypersensitivity.

#### Conflict of interest

The authors declare no conflict of interest.

#### Acknowledgements

This work was supported by grants from the National Natural

Science Foundation (81272042).

#### Appendix A. Supplementary material

Supplementary data associated with this article can be found in the online version at <http://dx.doi.org/10.1016/j.redox.2016.09.004>.

#### References

- [1] S. Staaf, S. Oerther, G. Lucas, J.P. Mattsson, P. Ernfors, Differential regulation of TRP channels in a rat model of neuropathic pain, *PAIN* 144 (2009) 187–199.
- [2] W. Kallenborn-Gerhardt, K. Schroder, T.D. Del, R. Lu, K. Kynast, J. Kosowski, E. Niederberger, A.M. Shah, R.P. Brandes, G. Geisslinger, A. Schmidtke, NADPH oxidase-4 maintains neuropathic pain after peripheral nerve injury, *J. Neurosci.* 32 (2012) 10136–10145.
- [3] J.Y. Moon, S.R. Choi, D.H. Roh, S.Y. Yoon, S.G. Kwon, H.S. Choi, S.Y. Kang, H. J. Han, H.W. Kim, A.J. Beitz, S.B. Oh, J.H. Lee, Spinal sigma-1 receptor activation increases the production of D-serine in astrocytes which contributes to the development of mechanical allodynia in a mouse model of neuropathic pain, *Pharmacol. Res.* 100 (2015) 353–364.
- [4] R.B. Griggs, R.R. Donahue, B.G. Adkins, K.L. Anderson, O. Thibault, B.K. Taylor, Pioglitazone inhibits the development of hyperalgesia and sensitization of spinal nociceptive neurons in type 2 diabetes, *J. Pain* (2015).
- [5] P. Zabielski, I.R. Lanza, S. Gopala, H.C. Holtz, H.R. Bergen, S. Dasari, K.S. Nair, Altered skeletal muscle mitochondrial proteome as the basis of disruption of mitochondrial function in diabetic mice, *Diabetes* (2015).
- [6] L. Valek, M. Kanngiesser, A. Haussler, N. Agarwal, C.H. Lillig, I. Tegeder, Redoxins in peripheral neurons after sciatic nerve injury, *Free Radic. Biol. Med* 99 (2015) 581–592.
- [7] J. Yowtak, K.Y. Lee, H.Y. Kim, J. Wang, H.K. Kim, K. Chung, J.M. Chung, Reactive oxygen species contribute to neuropathic pain by reducing spinal GABA release, *Pain* 152 (2011) 844–852.
- [8] W. Kallenborn-Gerhardt, K. Schroder, G. Geisslinger, A. Schmidtke, NOXious signaling in pain processing, *Pharm. Ther.* 137 (2013) 309–317.
- [9] W. Kallenborn-Gerhardt, S.W. Hohmann, K.M. Syhr, K. Schroder, M. Sisignano, A. Weigert, J.E. Lorenz, R. Lu, B. Brune, R.P. Brandes, G. Geisslinger, A. Schmidtke, Nox2-dependent signaling between macrophages and sensory neurons contributes to neuropathic pain hypersensitivity, *Pain* 155 (2014) 2161–2170.
- [10] H. Suzuki, N. Hatano, Y. Muraki, Y. Itoh, S. Kimura, H. Hayashi, K. Onozaki, Y. Ohi, A. Haji, K. Muraki, The NADPH oxidase inhibitor diphenyleneiodonium activates the human TRPA1 nociceptor, *Am. J. Physiol. Cell Physiol.* 307 (2014) C384–C394.
- [11] M. Ibi, K. Matsuno, D. Shiba, M. Katsuyama, K. Iwata, T. Takehi, T. Nakagawa, K. Sango, Y. Shirai, T. Yokoyama, S. Kaneko, N. Saito, C. Yabe-Nishimura, Reactive oxygen species derived from NOX1/NADPH oxidase enhance inflammatory pain, *J. Neurosci.* 28 (2008) 9486–9494.
- [12] S.R. Choi, D.H. Roh, S.Y. Yoon, S.Y. Kang, J.Y. Moon, S.G. Kwon, H.S. Choi, H. J. Han, A.J. Beitz, S.B. Oh, J.H. Lee, Spinal sigma-1 receptors activate NADPH oxidase 2 leading to the induction of pain hypersensitivity in mice and mechanical allodynia in neuropathic rats, *Pharmacol. Res.* 74 (2013) 56–67.

- [13] H. Sumimoto, K. Miyano, R. Takeya, Molecular composition and regulation of the Nox family NAD(P)H oxidases, *Biochem Biophys. Res. Commun.* 338 (2005) 677–686.
- [14] Y.B. Im, M.K. Jee, J.I. Choi, H.T. Cho, O.H. Kwon, S.K. Kang, Molecular targeting of NOX4 for neuropathic pain after traumatic injury of the spinal cord, *Cell Death Dis.* 3 (2012) e426.
- [15] V. Vitko-Sarsat, M. Friedlander, C. Capellere-Blandin, T. Nguyen-Khoa, A. T. Nguyen, J. Zingraff, P. Jungers, B. Descamps-Latscha, Advanced oxidation protein products as a novel marker of oxidative stress in uremia, *Kidney Int.* 49 (1996) 1304–1313.
- [16] M. Kalousova, J. Skrha, T. Zima, Advanced glycation end-products and advanced oxidation protein products in patients with diabetes mellitus, *Physiol. Res.* 51 (2002) 597–604.
- [17] F. Xie, S. Sun, A. Xu, S. Zheng, M. Xue, P. Wu, J.H. Zeng, L. Bai, Advanced oxidation protein products induce intestine epithelial cell death through a redox-dependent, c-jun N-terminal kinase and poly (ADP-ribose) polymerase-1-mediated pathway, *Cell Death Dis.* 5 (2014) e1006.
- [18] M. Skvarilova, A. Bulava, D. Stejskal, S. Adamovska, J. Bartek, Increased level of advanced oxidation products (AOPP) as a marker of oxidative stress in patients with acute coronary syndrome, *Biomed. Pap. Med. Fac. Univ. Palacky. Olomouc Czech Repub.* 149 (2005) 83–87.
- [19] E.S. Cannizzo, C.C. Clement, K. Morozova, R. Valdor, S. Kaushik, L.N. Almeida, C. Follo, R. Sahu, A.M. Cuervo, F. Macian, L. Santambrogio, Age-related oxidative stress compromises endosomal proteostasis, *Cell Rep.* 2 (2012) 136–149.
- [20] X.F. Wei, Q.G. Zhou, F.F. Hou, B.Y. Liu, M. Liang, Advanced oxidation protein products induce mesangial cell perturbation through PKC-dependent activation of NADPH oxidase, *Am. J. Physiol. Ren. Physiol.* 296 (2009) F427–F437.
- [21] M. Nakanishi, K. Hata, T. Nagayama, T. Sakurai, T. Nishisho, H. Wakabayashi, T. Hiraga, S. Ebisu, T. Yoneda, Acid activation of Trpv1 leads to an up-regulation of calcitonin gene-related peptide expression in dorsal root ganglion neurons via the CaMK-CREB cascade: a potential mechanism of inflammatory pain, *Mol. Biol. Cell* 21 (2010) 2568–2577.
- [22] M. Naziroglu, B. Cig, C. Ozgul, Neuroprotection induced by N-acetylcysteine against cytosolic glutathione depletion-induced Ca<sup>2+</sup> influx in dorsal root ganglion neurons of mice: role of TRPV1 channels, *Neuroscience* 242 (2013) 151–160.
- [23] M. Naziroglu, B. Cig, C. Ozgul, Modulation of oxidative stress and Ca(2+) mobilization through TRPM2 channels in rat dorsal root ganglion neuron by *Hypericum perforatum*, *Neuroscience* 263 (2014) 27–35.
- [24] L. Hou, X. Wang, PKC, PKA, but not PKG mediate LPS-induced CGRP release and [Ca(2+)]<sub>i</sub> elevation in DRG neurons of neonatal rats, *J. Neurosci. Res.* 66 (2001) 592–600.
- [25] H.Y. Li, F.F. Hou, X. Zhang, P.Y. Chen, S.X. Liu, J.X. Feng, Z.Q. Liu, Y.X. Shan, G. B. Wang, Z.M. Zhou, J.W. Tian, D. Xie, Advanced oxidation protein products accelerate renal fibrosis in a remnant kidney model, *J. Am. Soc. Nephrol.* 18 (2007) 528–538.
- [26] T. Druke, V. Witko-Sarsat, Z. Massy, B. Descamps-Latscha, A.P. Guerin, S. J. Marchais, V. Gausson, G.M. London, Iron therapy, advanced oxidation protein products, and carotid artery intima-media thickness in end-stage renal disease, *Circulation* 106 (2002) 2212–2217.
- [27] L. Kular, C. Rivat, B. Lelongt, C. Calmel, M. Laurent, M. Pohl, P. Kitabgi, S. Melik-Parsadaniantz, C. Martinerie, NOV/CCN3 attenuates inflammatory pain through regulation of matrix metalloproteinases-2 and -9, *J. Neuroinflamm.* 9 (2012) 36.
- [28] J.H. Zeng, Z.M. Zhong, X.D. Li, Q. Wu, S. Zheng, J. Zhou, W.B. Ye, F. Xie, X.H. Wu, Z.P. Huang, J.T. Chen, Advanced oxidation protein products accelerate bone deterioration in aged rats, *Exp. Gerontol.* 50 (2014) 64–71.
- [29] M. Shibasaki, M. Sasaki, M. Miura, K. Mizukoshi, H. Ueno, S. Hashimoto, Y. Tanaka, F. Amaya, Induction of high mobility group box-1 in dorsal root ganglion contributes to pain hypersensitivity after peripheral nerve injury, *PAIN* 149 (2010) 514–521.
- [30] M. Morell, M. Camprubi-Robles, M.D. Culler, L. de Lecea, M. Delgado, Cortistatin attenuates inflammatory pain via spinal and peripheral actions, *Neurobiol. Dis.* 63 (2014) 141–154.
- [31] S. Amadesi, J. Nie, N. Vergnolle, G.S. Cottrell, E.F. Grady, M. Trevisani, C. Manni, P. Geppetti, J.A. McRoberts, H. Ennes, J.B. Davis, E.A. Mayer, N.W. Bunnett, Protease-activated receptor 2 sensitizes the capsaicin receptor transient receptor potential vanilloid receptor 1 to induce hyperalgesia, *J. Neurosci.* 24 (2004) 4300–4312.
- [32] X.H. Liu, Q.Y. Zhang, L.L. Pan, S.Y. Liu, P. Xu, X.L. Luo, S.L. Zou, H. Xin, L.F. Qu, Y. Z. Zhu, NADPH oxidase 4 contributes to connective tissue growth factor expression through Smad3-dependent signaling pathway, *Free Radic. Biol. Med.* 94 (2016) 174–184.
- [33] U.S. Ozdemir, M. Naziroglu, N. Senol, V. Ghazizadeh, *Hypericum perforatum* attenuates spinal cord injury-induced oxidative stress and apoptosis in the dorsal root ganglion of rats: involvement of TRPM2 and TRPV1 channels, *Mol. Neurobiol.* 53 (2015) 3540–3551.
- [34] M. Ibi, K. Matsuno, D. Shiba, M. Katsuyama, K. Iwata, T. Kakehi, T. Nakagawa, K. Sango, Y. Shirai, T. Yokoyama, S. Kaneko, N. Saito, C. Yabe-Nishimura, Reactive oxygen species derived from NOX1/NADPH oxidase enhance inflammatory pain, *J. Neurosci.* 28 (2008) 9486–9494.
- [35] J. Qi, K. Buzas, H. Fan, J.I. Cohen, K. Wang, E. Mont, D. Klinman, J.J. Oppenheim, O.M. Howard, Painful pathways induced by TLR stimulation of dorsal root ganglion neurons, *J. Immunol.* 186 (2011) 6417–6426.
- [36] P. Martin-Gallan, A. Carrascosa, M. Gussinye, C. Dominguez, Biomarkers of diabetes-associated oxidative stress and antioxidant status in young diabetic patients with or without subclinical complications, *Free Radic. Biol. Med.* 34 (2003) 1563–1574.
- [37] F. Kosova, B. Cetin, M. Akinci, S. Aslan, Z. Ari, A. Sepici, N. Altan, A. Cetin, Advanced oxidation protein products, ferrous oxidation in xylenol orange, and malondialdehyde levels in thyroid cancer, *Ann. Surg. Oncol.* 14 (2007) 2616–2620.
- [38] J. Zuwala-Jagiello, M. Pazgan-Simon, K. Simon, M. Marwas, Advanced oxidation protein products and inflammatory markers in liver cirrhosis: a comparison between alcohol-related and HCV-related cirrhosis, *Acta Biochim. Pol.* 58 (2011) 59–65.
- [39] M.A. Eskander, S. Ruparel, D.P. Green, P.B. Chen, E.D. Por, N.A. Jeske, X. Gao, E. R. Flores, K.M. Hargreaves, Persistent Nociception Triggered by Nerve Growth Factor (NGF) Is Mediated by TRPV1 and Oxidative Mechanisms, *J. Neurosci.* 35 (2015) 8593–8603.
- [40] X. Xiao, X.T. Zhao, L.C. Xu, L.P. Yue, F.Y. Liu, J. Cai, F.F. Liao, J.G. Kong, G.G. Xing, M. Yi, Y. Wan, Shp-1 dephosphorylates TRPV1 in dorsal root ganglion neurons and alleviates CFA-induced inflammatory pain in rats, *Pain* 156 (2015) 597–608.
- [41] W. Ma, J.G. Chabot, F. Vercauteren, R. Quirion, Injured nerve-derived COX2/PGE2 contributes to the maintenance of neuropathic pain in aged rats, *Neurobiol Aging* 31 (2010) 1227–1237.
- [42] N. Malek, A. Pajak, N. Kolosowska, M. Kucharczyk, K. Starowicz, The importance of TRPV1-sensitisation factors for the development of neuropathic pain, *Mol Cell Neurosci.* 65 (2015) 1–10.
- [43] H.J. Weng, K.N. Patel, N.A. Jeske, S.M. Bierbower, W. Zou, V. Tiwari, Q. Zheng, Z. Tang, G.C. Mo, Y. Wang, Y. Geng, J. Zhang, Y. Guan, A.N. Akopian, X. Dong, Tmem100 is a regulator of TRPA1-TRPV1 complex and contributes to persistent pain, *Neuron* 85 (2015) 833–846.
- [44] Z. Dai, J. Xiao, S.Y. Liu, L. Cui, G.Y. Hu, D.J. Jiang, Rutaecarpine inhibits hypoxia/reoxygenation-induced apoptosis in rat hippocampal neurons, *Neuropharmacology* 55 (2008) 1307–1312.
- [45] M.L. Porto, L.M. Lirio, A.T. Dias, A.T. Batista, B.P. Campagnaro, J.G. Mill, S. S. Meyrelles, M.P. Baldo, Increased oxidative stress and apoptosis in peripheral blood mononuclear cells of fructose-fed rats, *Toxicol. Vitro.* 29 (2015) 1977–1981.
- [46] J.C. Wang, Y. Zhao, S.J. Chen, J. Long, Q.Q. Jia, J.D. Zhai, Q. Zhang, Y. Chen, H. B. Long, AOPPs induce MCP-1 expression by increasing ROS-mediated activation of the NF-kappaB pathway in rat mesangial cells: inhibition by sesquiterpene lactones, *Cell Physiol. Biochem.* 32 (2013) 1867–1877.
- [47] G. Rong, X. Tang, T. Guo, N. Duan, Y. Wang, L. Yang, J. Zhang, X. Liang, Advanced oxidation protein products induce apoptosis in podocytes through induction of endoplasmic reticulum stress, *J. Physiol. Biochem.* 71 (2015) 455–470.
- [48] M. Bordignon, D.L. Da, L. Marinelli, G. Gabai, Advanced oxidation protein products are generated by bovine neutrophils and inhibit free radical production in vitro, *Vet. J.* 199 (2014) 162–168.
- [49] W. Kallenborn-Gerhardt, R. Lu, K.M. Syhr, J. Heidler, H. von Melchner, G. Geisslinger, T. Bangsow, A. Schmidtko, Antioxidant activity of sestrin 2 controls neuropathic pain after peripheral nerve injury, *Antioxid. Redox Signal* 19 (2013) 2013–2023.
- [50] X. Cao, S.L. Demel, M.T. Quinn, J.J. Galligan, D. Kreulen, Localization of NADPH oxidase in sympathetic and sensory ganglion neurons and perivascular nerve fibers, *Auton. Neurosci.* 151 (2009) 90–97.
- [51] M. Naziroglu, A.C. Uguz, O. Ismailoglu, B. Cig, C. Ozgul, M. Borcak, Role of TRPM2 cation channels in dorsal root ganglion of rats after experimental spinal cord injury, *Muscle Nerve* 48 (2013) 945–950.
- [52] S.S. Stojilkovic, Ca<sup>2+</sup>-regulated exocytosis and SNARE function, *Trends Endocrinol. Metab.* 16 (2005) 81–83.
- [53] X. Qin, Y. Wan, X. Wang, CCL2 and CXCL1 trigger calcitonin gene-related peptide release by exciting primary nociceptive neurons, *J. Neurosci. Res.* 82 (2005) 51–62.
- [54] S. Benemei, P. Nicoletti, J.G. Capone, P. Geppetti, CGRP receptors in the control of pain and inflammation, *Curr. Opin. Pharmacol.* 9 (2009) 9–14.
- [55] A.M. Salmon, M.I. Damaj, L.M. Marubio, M.P. Epping-Jordan, E. Merlo-Pich, J. P. Changeux, Altered neuroadaptation in opiate dependence and neurogenic inflammatory nociception in alpha CGRP-deficient mice, *Nat. Neurosci.* 4 (2001) 357–358.
- [56] H.A. McDonald, T.R. Neelands, M. Kort, P. Han, M.H. Vos, C.R. Faltynek, R. B. Moreland, P.S. Puttfarcken, Characterization of A-425619 at native TRPV1 receptors: a comparison between dorsal root ganglia and trigeminal ganglia, *Eur J. Pharmacol.* 596 (2008) 62–69.
- [57] K. Ouyang, H. Zheng, X. Qin, C. Zhang, D. Yang, X. Wang, C. Wu, Z. Zhou, H. Cheng, Ca<sup>2+</sup> sparks and secretion in dorsal root ganglion neurons, *Proc. Natl. Acad. Sci. USA* 102 (2005) 12259–12264.